MATHEMATICAL MODELING OF A 500 W_e POWER MODULE COMPOSED BY A PEM FUEL CELL COMBINED WITH A DC-DC ENHANCED POTENTIAL OUTPUT CONVERTER

Roque Machado de Senna [(a)], Marcelo Linardi [(a)], Douglas Alves Cassiano[(b)], Ivan Santos [(a)], Edgar Ferrari da Cunha [(a)], Henrique de Senna Mota [(a)], Rosimeire Aparecida Jerônimo[(c)].

[(a)] Instituto de Pesquisas Energéticas e Nucleares - Universidade de São Paulo - IPEN/USP. Av. Lineu Prestes, 2242, Cidade Universitária, São Paulo, SP, Brasil, CEP05508-000
[(b)] Universidade Federal do ABC. Rua Santa Adélia, 166, Bangu, Santo André, SP, Brasil, CEP09210-170.
[(c)] Universidade Federal de São Paulo, Rua Prof. Artur Riedel, 275, Eldorado, Diadema, SP, Brasil, CEP09972-270.

[(a)]rmdesenna@usp.br, [(b)]douglas.cassiano@ufabc.edu.br, [(c)]rosijeronimo@yahoo.com.br

ABSTRACT

This work presents the development of a mathematical modeling of a 500 W_e PEMFC fuel cell stack (MCC500) system combined with a dc-dc enhanced potential output converter. The MCC500 was developed at IPEN (Nuclear and Energy Research Institute) and the company Electrocell, using Brazilian technology exclusively. Mathematical developments and modeling have been performed, relying on experimental data collected at IPEN laboratory. The first step was to prepare an electrical system (pre-design) for the proposed model, which included the MCC500 parameters, like: membrane ohmic resistance, activation resistance, electric double layer capacitance, open circuit potential, as well as DC-DC converter parameters, like the inductor and the transistor switching frequencies. Using the obtained parameters and a linear differential equation system with some mathematical manipulations, an electrical system model was determined. Simulations experiments demonstrated that the system was very stable. This contribution showed to be very important tool to generate useful potential for practical purposes, increasing the overall system electrical efficiency.

Keywords: Fuel Cell and Hydrogen. Fuel Cells System Model. Energy Efficiency. Mathematical Modeling.

1. INTRODUCTION

Electricity, as well as all other energy forms, has played a strategic role at the population life quality indicators, increasing every day in importance (Adam 1991).

Despite its huge social and economic relevance all activities related to energy exploration, production, distribution and use cause environmental impacts, concerning the substances that can release into the atmosphere, the water sources and the soil, endangering the health and survival any terrestrial ecosystem. The various energy systems steps are closely related to each other and to all mankind development.

There is a growing need to find solutions to the related negative effects of the energy production processes chain, with goals to minimize the social, environmental and economic injuries (Szwarc 2007).

The desirable characteristics for power sources are: clean, renewable, low noise emission, low operating costs, reliability, among the others desirable characteristics. Among the options for power sources from renewable sources and environmentally sustainable is the hydrogen gas, which has been used as an energy vector therefore, it is electricity energy storage for many energy sources types, it can be obtained from several energy processes (Linardi, 2010). Three main options may be addressed:

1. The first is the hydrogen production by water electrolysis, from use the electricity production excess from photovoltaic panels, wind generators, hydro, geothermal and nuclear power plants.

2. The second, through the energy use from biomass gasification and further purification, such as garbage, sewage, as well as the forest production remains, agribusiness and agriculture.

3. The third energy process, which has found a higher economic viability in the present day, is supported on catalytic reforming and gasification processes that lead to improved efficacy and reduce the fuel pollution potential already in use, such as ethanol, biodiesel, coal, oil and natural gas. The Brazil Hydrogen production tends to grow building on bioethanol (Brown, 2001), (Liguras et al., 2004; Vaidya and Rodrigues, 2006; Linardi, 2010).

An option for power generation, supported on hydrogen is the power module of PMFC Fuel Cells technology-

based. According to the DOE's Fuel Cell Technologies Market Report (DOE, 2011), PEM fuel cells ranging from 0.5 kW to 2 kW were suitable and indicated for residential applications, such as uninterruptible power supply and for combined heat and power supplying. Since the 2010 decade, 0.5 kW to 2 kW PEM fuel cell modules were available in the market, being commercialized for these stationary applications by Horizon and ClearEdge Power, among other companies. The choice of Mathematical Modeling developed for the 500 W PEMFC module in this present work was determined by these facts, although there were also recent mobile applications for this fuel cells class reported on the literature (Shang and Pollet, 2010).

These facts attest that it is extremely necessary to detail further systems studies, like developments based on fuel cells power modules and other renewable and environmentally sustainable technologies (Schoots *et. al.* 2010).

2. OBJECTIVES

The two main objectives of this work are:

1. Development of a mathematical modeling for a system including a PEM fuel cell stack (MCC500) combined to a dc-dc enhanced potential output.
2. Perform simulations using the mathematical model in order to enable the dc-dc converter to raise the bus potential and keep it constant, through the computer simulation on Matlab7® (Mathworks 2007).

3. STATE OF THE ART

3.1 The PEM Fuel Cell Stack - MCC500

The fuel cell is a direct electrochemical power converter (Wendt *et. al.* 2002). At a PEM fuel cell type, two half-cell reactions occur simultaneously, with an oxidation reaction (losing electrons) at the anode and a reduction reaction (gaining electrons) at the cathode.

These two reactions account for the oxidation-reduction reactions at the device, resulting in water formation, due to external fed gaseous hydrogen and oxygen combination, releasing thermal and electrical energy, this one flowing to an external circuit (Kinoshita 2001).

At the anode, the hydrogen molecules come into contact to the platinum catalyst sites (adsorption) on the gas diffusion electrode surface. The hydrogen molecules break their bonds at the platinum surface to form weak links H-Pt. Each hydrogen atom loses its electron to an external circuit, connected to a load, to meet the oxygen ions at the cathode. In turn, the hydrogen ions associated with water (H_3O^+) passes through the proton exchange membrane, reaching the cathode (Linardi 2010).

At the cathode, the oxygen molecules come into contact with the platinum catalyst on the gas diffusion electrode surface. The Oxygen molecules adsorb at the platinum electrode surface, where the oxygen-oxygen bond (O-O) is weakened, and so conditions for the reduction reaction are created. Each oxygen atom then combines with two electrons and two hydrogen ions to form a water molecule. The platinum catalyst at the cathode gas diffusion electrode is now free to weaken new oxygen molecules bonds (Spinacé 2003).

Practical system design requires higher power output than available in a single cell, accordingly, several cells in series association is necessary, named stack, as shown on figure 1, to reach this requirement.

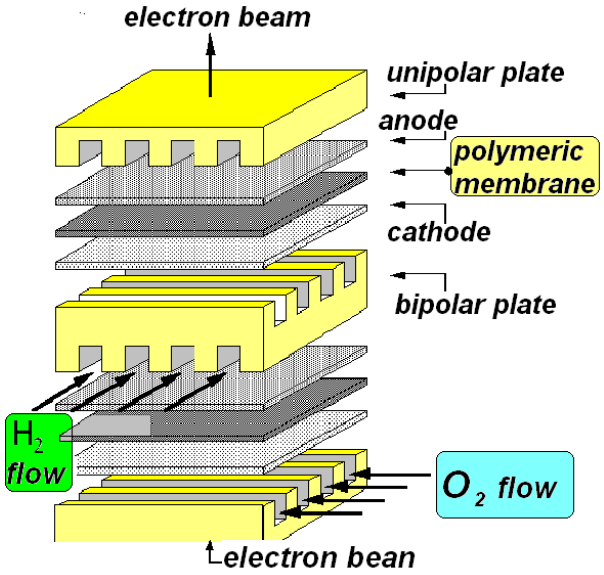

Figure 1: Schematic PEM Fuel Cell Stack (Adapted From Kinoshita 2001).

3.2 The MCC500 Developed at IPEN

The called MCC500 system, as shown at figure 2, is a stack composed by 10 single fuel cells in a series association. The produced electrodes could have, each, until 144 cm^2 of geometrical area, depending on the employed technology. In this work 10 electrodes of 144 cm^2 area were fabricated by the IPEN-Screen Printing Method (Boniface 2011), to be applied to the MCC500 system.

The IPEN-Alcohol Reducing Process was used to produce the Pt/C nano structured electrocatalysts in the gas diffusion electrodes (anode and cathode) (Spinacé 2003).

For the bipolar plates design, a computational simulation of fluid dynamics on gas flow channels was used (Cunha 2009).

In this way, a pre-commercial 500 W_e PEMFC power module was developed, as support for the distributed electricity generation industry, using only Brazilian technology. The Brazilian company ELECTROCELL also contributed to the stack design;

bipolar plate production; sealing, cooling systems and cells assembly.

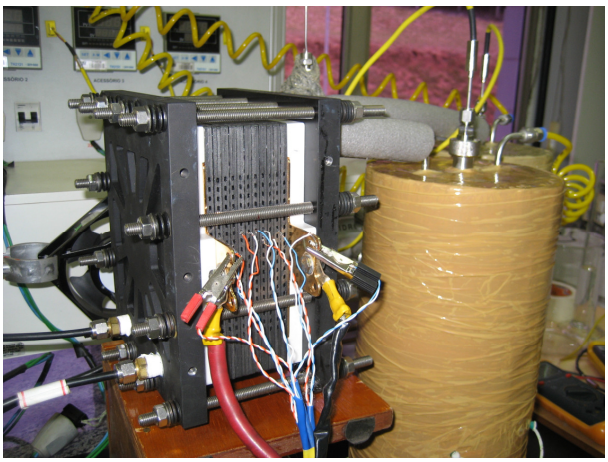

Figure 2: MCC500 Photography Developed at the IPEN and Electrocell® Laboratories.

Previous MCC500 tests showed stable operation, achieving the output power of 500 W_e (77.7 A, current at 6.43 V). The device also showed to be able to produce a maximum power of 574 W_e. For heat recovery studies, it was estimated that the thermal power output developed by MCC500 was 652 W_t, at 500 W_e nominal power. The total stack materials cost was estimated to be around US$ 2,531.70 (Cunha 2009).

3.3 DC-DC Step-up Converter with Enhanced Potential Output Converter

The DC-DC converter is able to receive the electrical potential produced (generated) at MCC500 and make it available on relatively stable potential for the load use, and thereby improve the conversion efficiency, especially when demand is high and the potential generated are small, as shown on Figure 3.

4 METHODOLOGY

4.1 Stability Analysis

In the development of stability analysis, two forms of Nyquist Methods were used. The simulation using Matlab7® computational program proved to be very effective in determining system behavior and in allowing the evaluation of either the output potential elevation or the computational disturbance stability. The system showed to be very stable both by the characteristic equation Root Locus Analysis and by the Nyquist Mapping Theorem (Jonckheere *et. al.* 2002).

4.2 The Mathematical Model Development of the DC-DC Enhanced Potential Output Converter (DC- DC Step-up Converter)

The dc-dc converter mathematical modelling began with a preliminary design of an electrical system, requiring additional steps, as follows:

1. Elaboration of the required polarization curve from current and potential measurements on the MCC500 stack, as shown by Figure 3.
2. Determination of the stood up parameters: inductance of the DC-DC converter inductor (L); the MCC500 electric double layer capacitance (C); the MCC500 membrane ohmic resistance (R_1); the MCC500 resistance activation (R_2), open circuit potential (E), as shown by Figure 4.
3. Combination of the parameters using some mathematical manipulations and the linear differential equations system, combined with mathematical calculations and module parameters (SR-12, Avista Labs). These data permit the electrical system lifting and support the parameterized circuit diagram form for the model presented, as shown by Figure 4 and table 1.

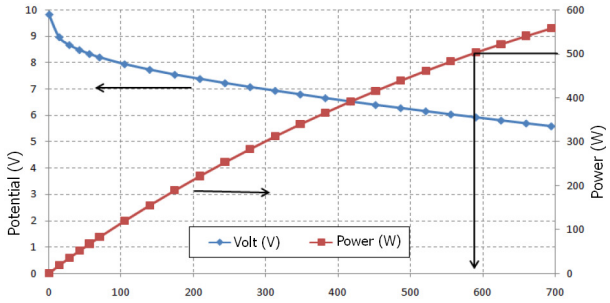

Figure 3: The PEM Fuel Cell Stack - MCC500 Polarization and Power Curves, (Adapted from Cunha 2009).

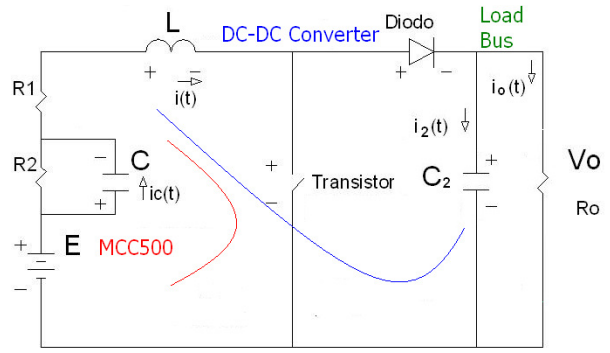

Figure 4: Schema of the Electrical Model for the MCC500 with Dc-Dc Converter, Parameterized to Control the Load Bus Potential, Author.

4.3 Simulation of the Converter Potential to Increase Capacity and Keep it Constant

This step was started by defining to apply the steps and pulses number. Then the program routine was developed and the assisted simulations on Matlab7® were carried out, culminating with the graphic form and table to results presentation.

5 RESULTS AND DISCUSSION

5.1 Determining the inductor to the system

The inductor (L) was obtained based on the equations (1) to (6) as described by Ahmed (2000) and Linardi (2010), and the data in the table (1) and (2), where (T_{on}) corresponds to half the period of the transistor switching frequency (fsh), (T) was period of the transistor switching frequency, (E_{op}) was the value of the standard potential operation, (I_{pp}) was the current ripple that was allowed the peak to peak for the inductor, (g_e) was the static gain, (D) was the commutation duty cycle, (Vi) was the linear initial potential, (L_{min}) was the minimum inductor value for warranting continuous current conduction into the diode, (R_o) was the load nominal resistance, and (V_o).was the stable potential in load bus.

$$g_e = \frac{V_o}{V_i} \tag{1}$$

$$D = \frac{g_e - 1}{g_e} \tag{2}$$

$$T_{on}(s) = D.T \tag{3}$$

$$L_{min}(H) = \frac{R_o . T_{on} . (1 - D)^2}{2} \tag{4}$$

$$L(H) = \frac{E_o . T_{on}}{I_{pp}} \tag{5}$$

Table 1: Date of the SR12, Avista Labs

Technology	PEMFC
MEAs	48
Open Circuit Potential (Module)	48 V
Electric Double Layer Capacitance	0.015F
Electric Double Layer Mean Charge	0.72 C
Nominal Power	500 We

Table 2: Date of the MCC500 and Electrical Model

Technology	PEMFC
MEAs	10
Area	144 cm^2
Nominal Power	500 We
Open Circuit Potential (Module) E	9.8 V
Nominal Potential (Module)	6.43 V
Potential (Regulated) in load bus V_o	14.4 V
Linear Low Potential V_L	5.3 V
Nominal Current (Module)	77.7 A
Load Mean Current I_o	34.6 A
Potential static gain g_e	2.7
Efficiency	43.4%
Operating Temperature	65 ° C
Electrolyte Resistance R_1	29.1 mΩ
Activation Resistance R_2	14.9 mΩ
Load Resistance R_o	417.7 mΩ
Load Capacitor C_2	0.005F
Electric Double Layer Capacitance C	0.0367F
Inductor L_{min}	360 pH
Inductor L	228 µH
Transistor Switching Frequency Period T	20 µs
Transistor Switching Frequency Period T_{on}	12.6 µs
Duty Cycle D	0.63

5.2 The Electrical Model

The electrical model is based on the inductor current coming from the MCC500 module, as shown by figure 4.

The six system equations on the time domain (t) and one equation on the complex domain frequency (s) were provided. Results were then obtained as described on the following steps:

Equation 7 inserted the increase due the modification in duty cycle (complementary, D' and d'(t)) on the transistor step or impulse by the controller;

$$D' = \frac{T_{off}}{T} \tag{6}$$

$$d'(t) = D' - \Delta d(t) \tag{7}$$

Equations 8 to 10 showed algebraically the change that occurred in the inductor current i (t) and in the regulated potential of load bus v_o (t) and in the electric double layer potential v_c (t) by the controller step or by impulse;

$$i(t) = I + \Delta i(t) \tag{8}$$

$$v_o(t) = V_o - \Delta v_o(t) \tag{9}$$

$$v_c(t) = V_c - \Delta v_c(t) \tag{10}$$

Equation 11 showed the MCC500 current in the electric double layer, due the potential variation by the variation during the time.

$$\frac{C \,.\, dv_c(t)}{dt} = i(t) - \frac{v_c(t)}{R_2} \tag{11}$$

Equation 12 showed the capacitor (C_2) current, due to the potential variation by to the variation during the time.

$$i_2(t) = \frac{C_2 \,.\, dv_o(t)}{dt} = d'(t) \,.\, i(t) - \frac{v_o(t)}{R_o} \tag{12}$$

Equation 13 showed the potential differences algebraic sum along the closed path, including C;

$$E - d'(t) \,.\, v_o(t) = \frac{L di(t)}{dt} + R_1 \, i(t) + v_c(t) \tag{13}$$

Equation 14 showed the MCC500 current in the electric double layer i_c (t) current, due to the potential variation by to the variation during the time.

$$i_c(t) = \frac{C \,.\, dv_c(t)}{dt} = i(t) - i_{R2}(t) \tag{14}$$

Equation 15 showed the MCC500 current in the electric double layer resistor (R_2), due the potential variation by the variation during the time.

$$i_{R2}(t) = \frac{v_c(t)}{R_2} \tag{15}$$

Equation 16 showed the switching frequency period (T), during the static duty cyrcle.

$$T(s) = T_{on} + T_{off} \tag{16}$$

The system composed by equations 1 to 16 is designed to support the Kirchhoff potentials law (the potential on closed path sum is always equal to zero), as described as by Nahvi and Edminister (2011). Equations 6 to 10 were obtained from Granville (1998). Equation 17 originated by solving the equations 7 to 16, wherein the DC terms, in the time (t) were excluded. Immediately after this operation was used Laplace transformation, and the result was showed in the frequency domain complex (s). Then, the terms have been grouped together as a function of (s), as showed in Literal Equations 17, and 17a to 17g, Close (1980) and Nahvi and Edminister (2011).

$$G(s) = \frac{\Delta v_o(s)}{\Delta d(s)} = \frac{V_0 \,.\, (n_1 + n_2 + n_3)}{D' \,.\, (d_1 + d_2 + d_3 + d_4)} \tag{17}$$

$$n_1 = s^2 \,.\, L \,.\, C \,.\, R_2 \tag{17a}$$

$$n_2 = s \,.\, \{ (D'^2 \,.\, R_o \,.\, C \,.\, R_2 - L - C \,.\, R_1 \,.\, R_2) \} \tag{17b}$$

$$n_3 = D'^2 \,.\, R_o - R_1 - R_2 \tag{17c}$$

$$d_1 = s^3.L.C.R_o.R_2.C_2 \quad (17d)$$

$$d_2 = s^2.(L.R_o.C_2+L.C.R_2+R_o.R_1.R_2.C.C_2) \quad (17e)$$

$$d_3 = s.(D'^2.R_o.C.R_2+L+R_1.R_2.C+R_o.R_1.C_2+R_o.R_2.C_2) \quad (17f)$$

$$d_4 = D'^2.R_o+R_1+R_2 \quad (17g)$$

Using this methodology, a transfer function was obtained coupling experimental data obtained from the power module and some mathematical transformation as shown by Figure 4 and tables 1and 2.

The final result is shown in equation 8.

$$G(s)_p=\frac{\Delta v_o(s)}{\Delta d(s)}=\frac{V_0.(n_1.n_2)}{D'.(d_1+d_2)} \quad (18)$$

$$n_1 = 25.3815.10^3 \quad (18a)$$

$$n_2 = s^2+s.1.8225.10^3+108.2598.10^3 \quad (18b)$$

$$d_1 = s^3+s^2.2.4352.10^3 \quad (18c)$$

$$d_2 = s.1.3536.10^6+286.1094.10^6 \quad (18d)$$

5.3 Simulations Using the Mathematical Model

The simulation performance result of mathematical model could be seen in Figure 5 and Table 3. Then to this it was used the mathematical model described in equation 18. It was shown that the end of 10 cycles of operation of the control system is increased the potential for the desired set value.

The horizontal axis indicates the time in seconds and the vertical axis the potential correction in volts, due the action of system control. The blue curve represents the response to a control step 0.0952 V applied to the first cycle of 50 kHz operation.

The simulation began with the definition of gains to be applied to the mathematical model, the potential sensor, the pulse width modulation controller (PWM). Then, it was adopted for the mathematical model the value of 0.095 V by the control step, in this case the gain of the plant model was 0.01G (s), and by way of simplification, the sensor and the gains of the controller PWM were modeled with unit values.

As shown in Table 3 it could be seen that in the course of 10 cycles, the system reaches the set point, showing that the setting adopted was successful.

As showed as on Figure 5 for the applied step, it can be seen that, from start, 90% of the additional set occurs on 2 ms (less than 60 Hz wave period), and the system is stable on 14 ms.

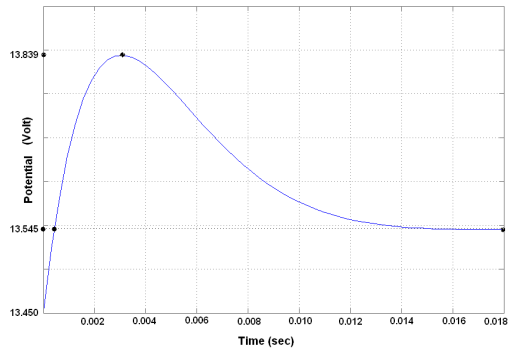

Figure 5: Performance of the controller to implement the first step to correct the potential to the controller. It was using the electrical model shown in equation 17, Author.

Table: 3 Mathematical Simulation of closed loop implementation and controller design

Cycle	Potential (V)	Reference (V)	Action
0	13.450	14.400	on
1	13.545	14.400	on
2	13.640	14.400	on
3	13.736	14.400	on
4	13.831	14.400	on
5	13.926	14.400	on
6	14.021	14.400	on
7	14.116	14.400	on
8	14.212	14.400	on
9	14.307	14.400	on
10	14.402	14.40	off

The basic feature of the transient response of a closed loop system depends on the closed loop poles location. If the system loop gain is variable, then the

location of the closed loop poles will depend on the loop gain value selected. Therefore it is important that the poles are known as closed-loop moving on the complex plane (s), as the loop gain varies, as shown in Figure 7.

The closed-loop poles are the roots of the characteristic equation. A method for determining the roots of a characteristic equation is called the root locus, and allows that the roots of the characteristic equation are represented graphically for all values of the system parameter. Usually the gain varies between zero and infinite.

Figure 7 was used to evaluate the stability of the DC-DC converter with the support of equation 18 and the graphical representation of the characteristic equation roots for the closed loop. Then, it can be concluded that this closed loop system is rather stable, because the roots of its characteristic equation stood in the left half of the s-plane (on the complex frequency domain), (Ogata 2011)

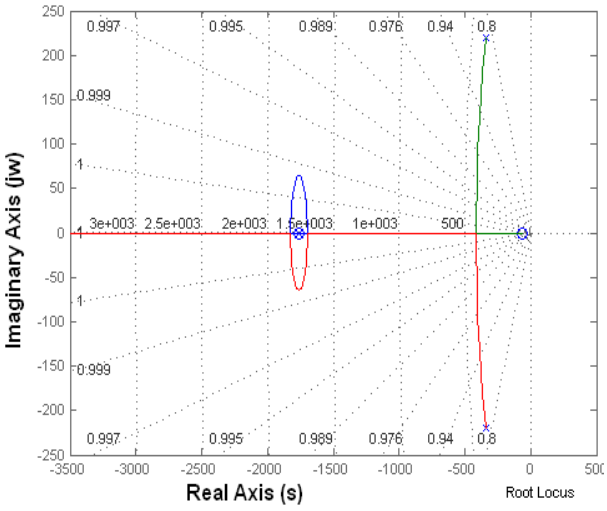

Figure 7: The Characteristic Equation Stability Analysis by the Root Locus Method, Author.

It is also useful to analyze the system using the Nyquist stability criteria for Mapping Theorem, which states that a closed loop system is stable if the outline of the entire right half of "s" (clockwise) with the frequency (w), varying from - ∞ to + ∞, on the imaginary axis (jw), there is no involvement on the origin path of the characteristic equation 18. At this situation there will be no poles and then the closed-loop system is stable. Also, Figure 8 is able to show that the system model is stable for graphical representation based on Nyquist path, because there is no engagement of the source (Ogata 2011).

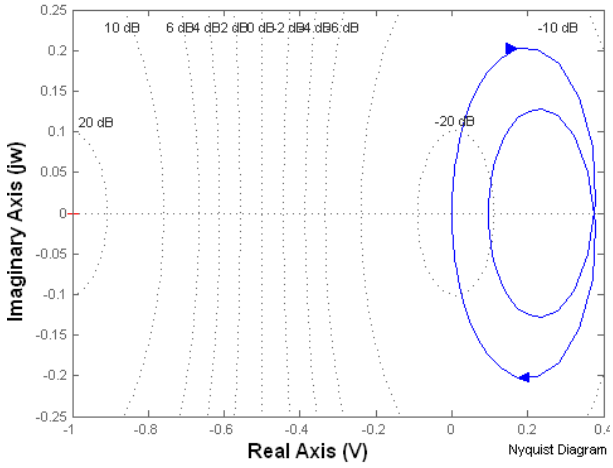

Figure 8: The Characteristic Equation Stability Analysis by the Nyquist Mapping Theorem, Author.

6 CONCLUSIONS

The developed system proved to be stable according to the Root Locus Method and Nyquist mapping theorem analyses performed.

The contribution given by the present developed model showed to be very important to generated useful potential for practical purposes, increasing the overall electrical efficiency, using the MCC500 system, built using Brazilian technology exclusively for stationary purposes power systems.

REFERENCES

Alam, M.S., Bala, B.K., Huq, A.M.Z., Matin, M.A., 1991. A Model for the Quality of Life as a Function of Electrical Energy Consumption. *Energy*, 16 (4), 739–745.

Bonifácio, R. N., Paschoal, J. O. A., Linardi, M. 2011. Catalyst Layer Optimization by Surface Tension Control During Ink Formulation of Membrane Electrode Assemblies in Proton Exchange Membrane Fuel Cell. *Journal of Power Sources, published by Elsevier,* 196, 4680-4685.

Brown, L. F., 2001. A Comparative Study of Fuels for On-Board Hydrogen Production for Fuel-Cell-Powered Automobiles, in*: International Journal of Hydrogen Energy*, 26(4), 381–397.

Close, M. C, 1980. *Circuitos Lineares.* 1980. 2nd edition, 550p, Rio de Janeiro, Brazil: LTC Editora.

Cunha, E. F., 2009. *Avaliação e Aplicação de Tecnologias de Células a Combustível Tipo PEMFC Desenvolvidas no IPEN em um Módulo de 500 We de Potência Nominal*. Thesis (PhD). Instituto de Pesquisas Energéticas e Nucleares - Universidade de São Paulo.

DOE - U.S. Department of Energy, 2011, Fuel Cell Technologies Market Report. U.S. Department of Energy publication, 68 p.

Friedrich, A., Carrette, L., Stimming, U., 2000. Fuel Cells: Principles, Types, Fuels, and Applications. *European Journal of Chemical Physics and Physical Chemistry*, 1(4), 162-193.

Granville, Smith, Longley, 1998. *Elementos de Cálculo Diferencial e Integral,* Edição Brasileira. Rio de Janeiro: Editora Científica.

Jonckheere, E. A., Coutinho, M. G. Chih-Yung Cheng, A., 2002. Computational Geometry Approach to Simplicial Nyquist Maps in Robust Stability, American Control Conference, Los Angeles, USA. *Proceedings of the American Control Conference Baltimora,* Maryland, June 1994. (213)740-4457

Kinoshita, K., 2001. *Electrochemical uses of carbon*. Available from : http://electrochem.cwru.edu/ encycl/art-c01-carbon.htm [accessed 23 March 2012].

Liguras D. K.; Goundani, K.; Verykios, X. E. 2004. Production of hydrogen for fuel cells by catalytic partial oxidation of ethanol over structured Ni catalysts, in: Journal of Power Sources, published by Elsevier, 130(1-2),30–37.

Linardi, M., 2010. *Introdução à Ciência e Tecnologia de Células a Combustível*. São Paulo: Artliber Editora.

Mathworks, 2007. *Matlab7/Simulink: Real-Time Workshop, TargetBox*. Available from: http://www.mathworks.com/ [accessed 18 October 2011]

Nahvi and Edminister, J., 2011. *Schaum's Outline of Electric Circuits,* Fifth Edition. São Paulo: Publisher: MCGRAW-HILL.

Ogata, K. *Modern Control Engineering*. USA, Prentice Hall Inc, 5th edition, 2011. 824p

Schoots, K., Kramer, G. J., Van Der Zwaan, B. C. C., 2010. Technology Learning for Fuel Cells: an Assessment of Past and Potential Cost Reductions. *Energy Policy*, 38(6), 2887-2897.

Shang, J. L., Pollet , B. G., 2010, Hydrogen fuel cell hybrid scooter (HFCHS) with plug-in features on Birmingham campus. International Journal of Hydrogen Energy, 35, 12709-12715.

Spinacé, E. Oliveira Neto, A., Linardi, M., 2003. Electro-Oxidation of Ethanol on PtRu/C Electrocatalysts Prepared from (n-C2H4)(Cl)Pt (uCl)2Ru(Cl)(n3, n3-C10H16). *Journal of Power Sources*, 124, 426-431.

Szwarc, A., 2007. *Bioenergia e Meio Ambiente.* Proceedings of Conferência Nacional de Bioenergia - BIOCONFE, USP. Available from: http://www.usp.br/bioconfe/downloads.htm [accessed 18 October 2011].

VAIDYA, P. D.; RODRIGUES, A. E. 2006. Insight into Steam Reforming of Ethanol to Produce Hydrogen for Fuel Cells, in: *Chemical Engineering Journal*, 117(1), 39-49.

Wendt, H.; Linardi, M.; Aricó, E. 2002. Células a Combustível de Baixa Potência Para Aplicações Estacionárias. *Química Nova*, 25, 470-476.